Construction of low-wettable free-standing layer-by-layer multilayer for fibrinogen adsorption

Kengo Manabe, Sabrina Belbekhouche

Construction of Low-Wettable Free-Standing Layer-by-Layer Multilayer for Fibrinogen Adsorption

Kengo Manabe,*,†,‡ Sabrina Belbekhouche**,§

†National Institute of Advanced Industrial Science and Technology (AIST), 1-2-1 Namiki, Tsukuba, Ibaraki 305-8564, Japan

‡Center for Material Design Science, School of Integrated Design Engineering, Keio University, 3-14-1 Hiyoshi, Kohoku-ku, Yokohama, Kanagawa 223-8522, Japan

§Institut de Chimie et des Matériaux Paris-Est, UMR 7182 CNRS-Université Paris-Est Créteil Val-de-Marne, 2 rue Henri Dunant, 94320 Thiais, France

Corresponding authors: Kengo Manabe,* Sabrina Belbekhouche**

Contact authors e-mail: kengo.manabe@aist.go.jp*, belbekhouche@icmpe.cnrs.fr**

KEYWORDS

free-standing films, layer-by-layer, self-assembly, protein adsorption, fibrinogen

ABSTRACT

With advancements in medical technology, various wound dressing materials are available for all types of wounds. As a dynamic process of wound healing, the first phase, namely “hemostasis” depending on protein adsorption, is a pivotal role for the following continuous phase. Although recent technological developments are investigating wound dressings that are degradable *in vivo* or thinner and less visible by fabricating a film that is free-standing from the substrate, there are few literatures which can show self-standing Layer-by-Layer (LbL) films dealing with the complex relation of mechanical property, wettability, and protein adsorption. Here, we demonstrate a wettability-controlled free-standing LbL multilayer with featuring each construction process. The successful free-standing LbL films were evaluated for efficient fibrinogen adsorption. The surface wettability was controlled by changing the number of bilayers and the annealing temperature as a process before peeled off from the substrate, and it increased from 40° to nearly 90°. The annealing time also influenced the peeling time by changing swelling and shrinkage, and the annealing at 180°C achieved the complete exfoliation from the substrate for 10 min. The 35-bilayer free-standing film showed the maximum stress value of 29.4 MPa and the elongation property of 2.2%. The free-standing LbL film trapped fibrinogen in the fibrinogen dispersion while the film without annealing did not show the change of peak ratio after the fibrinogen adsorbed test. The study would be valuable for manufacturing wettability-controlled free-standing films and demonstrate the possibility of future wound healing thin films.

INTRODUCTION

Skin is considered as the most exposed and the largest organ of a human body. The outer layer, epidermis composed of mainly keratin is a barrier for protection against viruses, pathogens, bacterial, and microbes as well as critical environment represented as chemical, thermal, mechanical dangerous conditions.[1] The skin is always an open door to physical damage and chemically damaging disorders such as medications, and exposure to them results in wounds that are not easily healed.[2,3] Wound healing is a complex and dynamic process that is completed by progressing tissue regeneration and growth through four sequential stages: hemostasis, inflammation, proliferation, and remodeling/maturation.[4,5] The skin is made up of vascular tissue and therefore has the ability to regenerate itself, but for skin damage above a certain level, the skin cannot regenerate without external support. The physicians distinguish and select between the various types of dressing materials by identifying the wound condition with an understanding of the healing process. Therefore, in the field of skin wound healing, various wound dressings have been studied as alternatives to mimic the skin for clinical solutions to promote healing.[6,7]

Sponges and gauze are practical wound dressing materials that are widely used not only in clinical practice but also in the home.[8,9] However, there are several problems with these off-the-shelf products, including the need for additional fixation in the damaged area, lack of flexibility, risk of infection, and the time required for surgery. On the other hand, from an academic perspective, scientists have been studying materials that mimic the functional and structural features of the skin's extracellular matrix, and that is thin like skin but have mechanical stability and elasticity.[10-12] In addition, a working hypothesis that has emerged as a surface science idea in wound dressing materials is that fibrinogen adsorption is the first step in the acute

biological response to engineered materials.[13] Therefore, the surface control has become one of the most important topics for future research on medical components. Controlling the surface can change the wettability of the surface, change the adsorption properties of the protein, and improve the cell adhesion, which is an effective means of altering the resulting biological interactions on the material.[14] Despite considerable efforts of the previous studies, however, these strategies usually include disadvantages such as poor protein adhesion in the case of composites, limited mechanical strength in the case of hydrogels, and lack of interconnectivity in the case of porous scaffolds.

To overcome these challenges, this study approaches free-standing films with controlling the wettability via layer-by-layer (LbL) self-assembly, which is a stable multilayer forming method.[15-19] The LbL self-assembly is based on the alternate adsorption of oppositely charged materials such as the electrostatic attraction of polymers.[20-22] It is a facile, versatile, cost-effective, and eco-friendly method that is performed at ambient temperature and pressure. Moreover, LbL self-assembly can allow the surface texture and thickness of the film to be controlled at micro- and nanoscales.[23-25] Films produced using this LbL self-assembly have been developed for various applications, represented as free-standing, optical antireflective/reflective, antifogging, superhydrophobic films, and drug delivery systems.[26-33] The free-standing system was developed using a sacrificial layer between a substrate and a LbL film that can exfoliate from the substrate by changing the pH value.[34] For wound dressings, it may be possible to develop thinner films with superior mechanical strength (and well stretched) by applying free-standing films. However, there are still few previous studies that can demonstrate free-standing LbL films that address the complex relationship between such mechanical properties, surface wettability, and protein adsorption.

The protein adsorption properties of LbL coatings composed of combinations of polymers exhibiting electrostatic interactions have been investigated in several previous studies.[35] Wittmer et al. evaluated the membrane adsorption of fibronectin, a matrix protein known to promote cell adhesion, in LbL membranes composed of poly(l-lysine) and dextran, and suggested that low hydration is effective for protein adsorption.[36] On the other hand, hydrophilic surfaces, such as those with zwitter surface and intermediate water, have been found to make it harder for proteins to adsorb to the surface.[37-39] Also, we have previously shown that a small percentage of hydroxyl groups adsorb proteins and promote thrombus formation, while LbL multilayers enriched with free hydroxyl groups are resistant to fibrinogen adsorption and antithrombotic performances.[40] The blood coagulation reaction begins with the adsorption of fibrinogen and undergoes a morphological change to fibrin. [39] This process of conversion from fibrinogen to fibrin is an irreversible reaction. Fibrinogen also plays an important role in blood coagulation in terms of its ability to adhere and aggregate platelets. Therefore, in this study, we promote the adsorption of fibrinogen, which is the most initiating step in the blood coagulation reaction, to achieve an effective wound dressing surface. Hence, our in vitro protein adsorption experiments were performed with fibrinogen.

Herein, the study demonstrates a guide to building free-standing films with the investigation of mechanical performance, chemical stability, and surface wettability. In order to propose an application of a free-standing film successfully fabricated by the LbL self-assembly method (strategy shown in Scheme 1), the protein adsorption properties of the free-standing membrane were evaluated. Cross-linking from hydrophilic materials via LbL self-assembly rather than hydrophobic materials and changing their surface features can allow precise control of film thickness and surface wettability, leading to free-standing fibrinogen adsorbed films with

more mechanical stability. As a result, it was found that fibrinogen was predominantly adsorbed on the free-standing film, indicating the possibility of its subsequent development into a healing process. This study suggests that the low-wettable free-standing LbL films may become a potential material to recover the functional and structural properties of damaged skin.

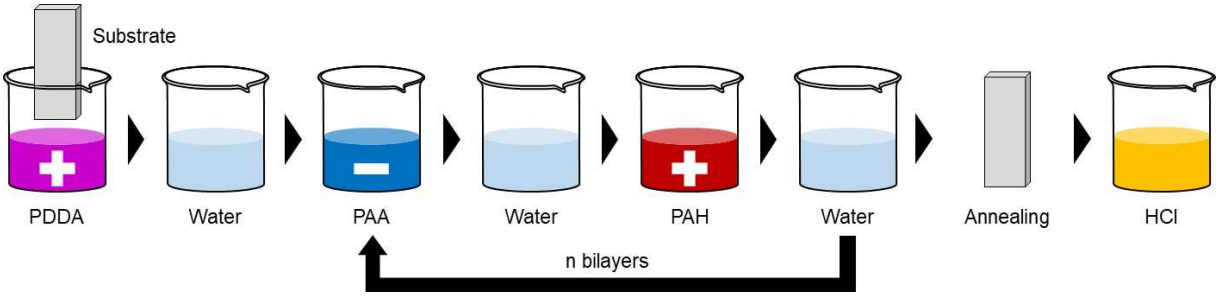

Scheme 1. Schematic image of the fabrication procedure for self-standing LbL films (PDDA: poly(diallyl dimethyl ammonium chloride), PAA: poly(acrylic acid), PAH: poly(allylamine hydrochloride) and HCl = hydrochloric acid).

MATERIAL AND METHODS

Materials. poly(diallyl dimethyl ammonium chloride) (PDDA; 20 wt.% aqueous solution, M_w ~ 400,000 – 500,000 g/mol, Sigma-Aldrich, St. Louis, MO, USA) as a cationic sacrificial layer, poly(allylamine hydrochloride) (PAH; powder, M_w ~ 70,000 g/mol, Sigma-Aldrich, St. Louis,

MO, USA) as a cationic layer, and poly(acrylic acid) (PAA; 35 wt.% aqueous solution, M_w ~ 400,000 – 500,000 g/mol, Sigma-Aldrich, St. Louis, MO, USA) as an anionic layer were used for the LbL film preparation. Slide glasses (76 × 26 mm^2, Matsunami Glass Ind., Ltd., Kishiwada, Japan) were used as substrates. For the protein adsorption test, fibrinogen (Wako Pure Chemical Industries, Ltd., Osaka, Japan) was selected.

Preparation of polyelectrolyte solutions. Solutions of PDDA, PAH, and PAA were prepared at a concentration of 1 mg/mL in deionized water and adjusted to pH 4.5, 7.5, and 3.5 with 5 M NaOH (Kanto Chemical Co., Inc., Tokyo, Japan), respectively. All aqueous solutions for LbL self-assembly were prepared with pure water (Aquarius GS-500.CPW, Advantec, Tokyo, Japan).

Free-standing LbL film preparation. LbL films were assembled on cleaned substrates using an automatic dipping machine. Substrates were cleaned with deionized water and a solution composed of 1 g of KOH / 120 g of H_2O / 160 g of isopropanol by dipping sequentially into deionized water for 5 min, KOH solution for 2 min, and then deionized water again for 5 min under ultrasonic cleaning. The glass substrates were initially coated with a thin buffer sacrificial layer composed of PDDA by immersing PDDA solution for 10 min and rinsing with deionized water three times for each 1 min. Then, LbL films with a bilayer architecture of (anionic polymer/cationic polymer)$_n$ were built, where n is the number of bilayers. The polycation solution was PAH, and the anionic solution was PAA. One bilayer was constructed by depositing a polyanion layer (10 min), followed by a polycation layer (10 min); a cascade water rinse cycle of three rinse baths for each 1 min was used (Scheme 1). The rinse baths were replaced and

refreshed every 10-bilayer to remove contaminants. After drying at 60°C for 1 min, the fabricated LbL films on the substrates were annealed at 160/180/200°C for 2 h for a thermal cross-linking. To exfoliate the films from the substrates, the LbL films on the substrates were immersed in HCl solution (Kanto Chemical Co., Inc., Tokyo, Japan) at pH 2.0, and then rinsed in pure water, resulting in free-standing LbL films.

Characterization. Surface morphology was observed by a laser scanning microscope (VK-9710, Keyence Corp., Osaka, Japan) and a field-emission scanning electron microscopy (FE-SEM; S-4700, Hitachi, Ltd., Tokyo, Japan). The film thickness of the fabricated LbL film was measured using a dektak (dektak-8000, Bruker Corp., Billerica, MA, USA). Surface wettability was characterized by the measurement of the contact angle of a 10-μL water droplet. The mechanical property of the films was investigated using a tensile testing machine (EZ-SX, Shimadzu Corp., Kyoto, Japan). The chemical bonds within the films before and after the thermal cross-linking were examined by Fourier transform infrared spectroscopy (FT-IR) (ALPHA-T, Bruker Corp., Billerica, MA, USA). To examine protein adsorption, fibrinogen dissolved in PBS (pH 7.3) to a concentration of 0.5 mg/mL, and the change of the chemical bond before and after immersing into the fibrinogen solution were measured by the FT-IR.

RESULTS AND DISCUSSION

Construction of stable free-standing LbL films.

LbL growth of the fabricated PAA/PAH films was measured by the dektak instrument. As shown in Figure 1, the PAA/PAH films showed an exponential thickness growth from 5- to 45-bilayer. According to the calculations from the graph, the increase was found to be by average 133 nm per 1-bilayer. Below 30-bilayer, the uniformity of the film is high and the deviation is small, while above 35-bilayer, the non-uniformity due to micro-order unevenness occurs and the deviation is large even in the same plane.

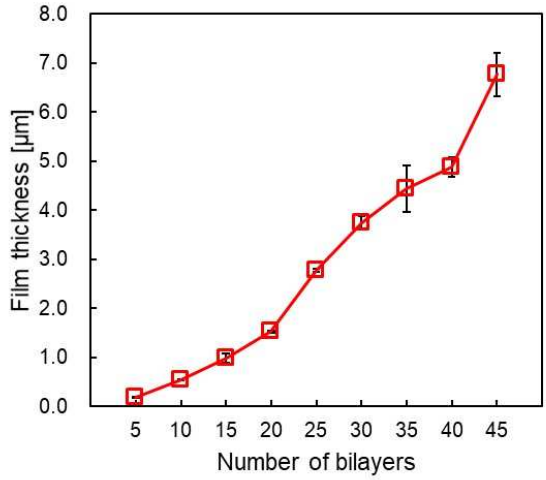

Figure 1. Relationship between the number of bilayers and film thickness of LbL films.

Since it was suggested that the non-uniformity of the films increases with the number of layers, the actual non-uniformity was evaluated by observing the surface structure of the fabricated films. The surface structure of the thin film was observed with the laser scanning microscope, which allows the evaluation of height displacement, and the results are shown in Figure 2. The laser microscopic images of the 35-bilayer and 45-bilayer show large unevenness.

The RMS values for each bilayer from the laser micrographs increased linearly (Figure 3), with the RMS growing to the micro-order above 35-bilayer. Thus, as the number of stacks increases, a surface structure emerges, increasing roughness, resulting in macroscopic inhomogeneity. In addition, the surface structure was evaluated by FE-SEM (Figure 2, second line). SEM images show that the surface structure of the 15-bilayer and 25-bilayer is almost unidentifiable. On the other hand, the 35-bilayer and 45-bilayer showed scattered agglomerates on the surface, especially the 45-bilayer, which showed clear agglomerate-like bumpy unevenness. These micro- and nano-level concave and convex structures increase the heterogeneity, which can be expected to change the surface wettability. A possible cause of the agglomeration and inhomogeneity is that the films are deposited by alternating layers of polymers due to electrostatic interactions, which results in the formation of poly-ion complexes in polymeric and water rinse solutions with increasing numbers of layers.

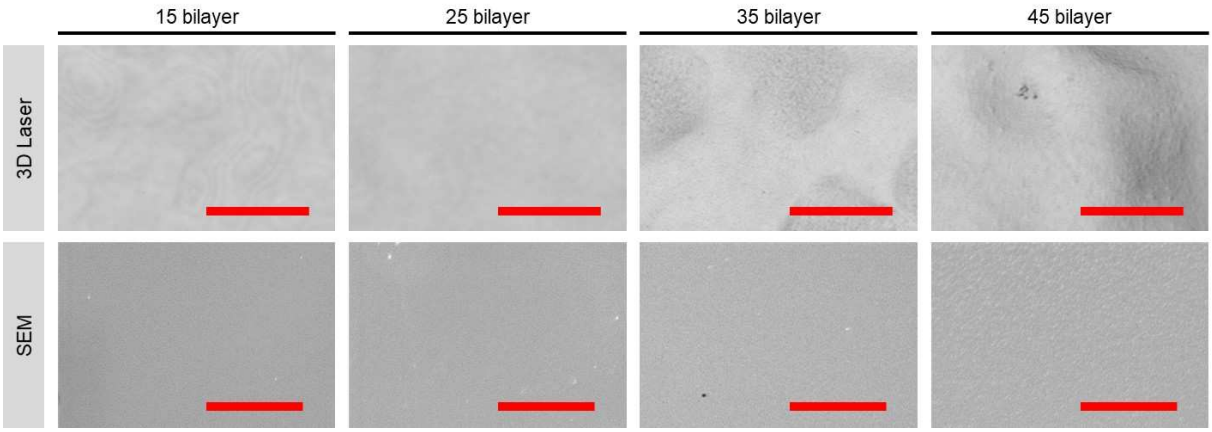

Figure 2. Laser scanning microscope images (first line) and FE-SEM images (second line) of LbL films with different numbers of bilayers. All scale bars in the images are 10 μm.

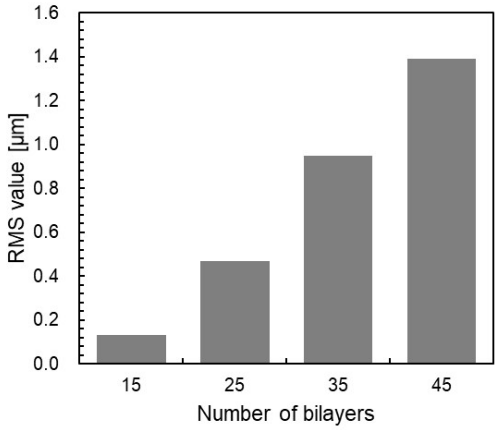

Figure 3. RMS value of LbL films with 15, 25, 35, and 45 bilayers.

Surface wettability, which is important for the evaluation of the surface properties of thin films, was investigated (Figure 4). The surface before annealing treatment showed hydrophilicity of less than 50° for all layers when the number of bilayers was changed. Up to 35-bilayer, the contact angle of water droplets increases, but there is not much increase between 35-bilayer and 45-bilayer. The reason for this is that the above-mentioned changes in the surface structure are due to the change between 25-bilayer and 35-bilayer. Next, we indirectly ascertain how the surface functional groups are altered by annealing treatment by evaluating how surface wettability changes with heat treatment. The contact angles increased with increasing the temperature of the annealing process for all the bilayers. The amide bonds between the carboxyl groups of PAA and the amino groups of PAH, which are components of the LbL film, are formed by thermal cross-linking, resulting in a decrease in the total carboxyl groups of the film and a shift to the hydrophobic side. [41,42] Especially at temperatures above 180°C, the contact angle approaches 90° due to changes in the concave and convex structure and chemical bonds of the membrane.

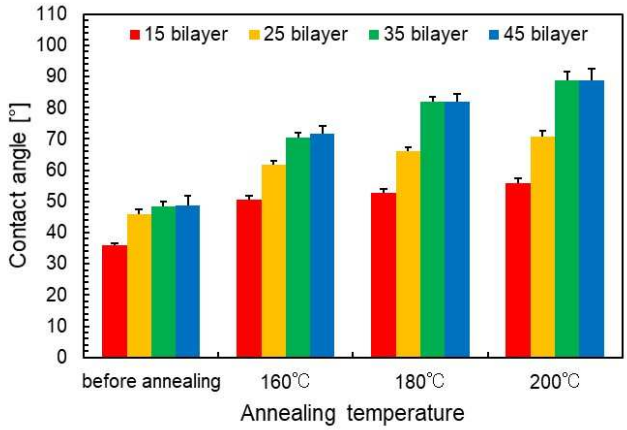

Figure 4. Water contact angle changes of LbL films with 15, 25, 35, 45 bilayers before and after annealing at 160, 180, 200°C.

The effect of crosslinking temperature on the exfoliation rate is investigated by observing the exfoliation process. As shown in Figure 5, in the case of a 35-bilayer film heated to 180°C, the entire film is stripped in about 10 min. In detail, after about 4 min, the film began to peel off from the edge of the substrate, and after about 8 min, the stripping solution penetrated to the central part of the film, and after about 10 min, the entire film was stripped from the substrate. The peeling time at which the film completely detached from the substrate was evaluated for each layer and each heat treatment temperature (Figure 6). Regardless of the number of bilayers, the rate of exfoliation tended to be faster as the temperature of thermal cross-linking increased. In thermal cross-linking, it is known that the higher the heating temperature, the higher the cross-linking progress, and the cross-linking level is 200°C > 180°C > 160°C.[43] The exfoliation method used in this study allows the PAA-PAH to form covalent bonds instead of electrical

interaction, and the electrical interaction between the sacrificial layer PDDA and PAA/PAH are deactivated by immersion in HCl solution to exfoliate the free-standing film. According to this principle, the more the cross-linking progress, the more the exfoliation progress. However, it was observed that the free-standing LbL film, which had been annealed at 200°C, broke or partially broke during the peeling process. As the thermal cross-linking progress, the entire membrane changes from hydrophilic to hydrophobic, as shown in the contact angle change described above. Therefore, when the film was immersed in the exfoliation solution, it was considered that the cracks entered at the chemically brittle points that affected the surface wettability. PAA/PAH membranes tend to swell with liquid, and H+ ions tend to enter into the membrane, suggesting that the LbL membrane itself, once contracted by annealing, is easy to swell.[44] Such swelling is the driving force for the separation between the substrate and the first layer of PDDA, and the separation progress easily. However, as the heating temperature increases and cross-linking progress, the degree of cross-linking increases, and swelling becomes less. One driving force for exfoliation is the increase in volume due to swelling, whereas at 200°C, considering the result that the exfoliation rate is fast but brittle, it is expected that the swelling relationship from shrinkage from thermal cross-linking to immersion in the exfoliation solution is the driving force for the overall exfoliation. Therefore, in the subsequent tests, the films were prepared and evaluated at 180°C with a fast peel time and no defects.

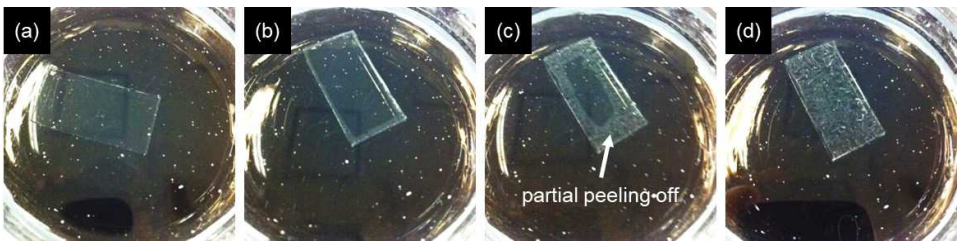

Figure 5. Exfoliation process of free-standing LbL films at (a) 0 min, (b) 4 min, (c) 8 min, and (d) 10 min.

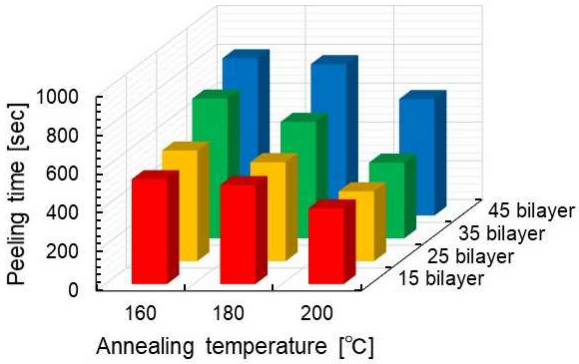

Figure 6. Peeling time of free-standing LbL films from the substrates with 15, 25, 35, and 45 bilayers after annealing at 160, 180, 200°C.

Tensile tests were performed on free-standing membranes of 15-, 25-, 35-, and 45-bilayer (Figures 7 and 8). Therefore, in the subsequent tests, the films were prepared and evaluated at 180°C with a fast peel time and no defects. The tensile strength of the free-standing membrane increased with the number of layers up to 15-bilayer ~ 35-bilayer. However, the tensile strength is reduced in 45-bilayer. This could be due to the effect of brittleness associated with an increase in the concave and convex structure of the membrane. The RMS value of the fabricated free-standing membranes increases with the number of stacks, which is caused by a large difference in the height of the unevenness in the membrane. Thus, in the case of thin films with different altitudes, there is a possibility that the unevenness and unevenness cause cracks and defects, causing the rupture. Also, as mentioned above, the unevenness of this film itself is thought to be

due to the presence of a large number of poly-ion complexes, which would reduce the tensile strength of the laminate because they would be a factor in the reduction of the adhesion of the laminate. The maximum stress and Young's modulus calculated from the tensile tester were 29.4 MPa with the elongation property of 2.2% and 27.4 MPa for the 35-bilayer, respectively, and the film was successfully fabricated with both flexibility and strength compared to other layers.

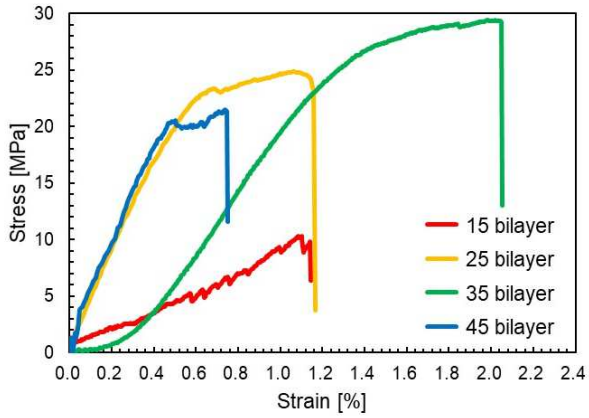

Figure 7. Stress-strain curve by tensile testing of free-standing LbL films with 15, 25, 35, and 45 bilayers.

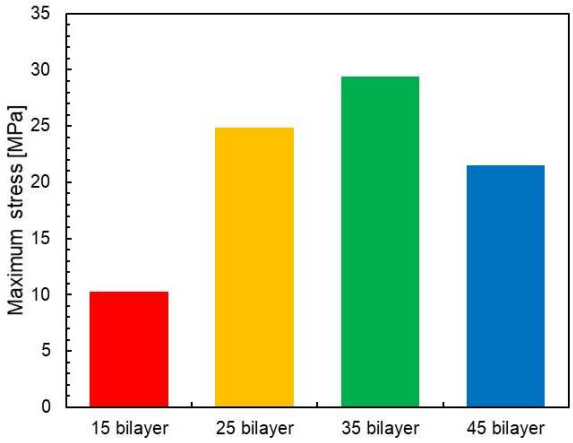

Figure 8. Maximum stress values by tensile testing of free-standing LbL films with 15, 25, 35, and 45 bilayers.

To define changes in chemical structures, FT-IR spectra were measured on the successful films with 35-bilayer before and after annealing (Figure 9). The FT-IR spectra of the films without annealing revealed the presence of a strong $–COO^-$ peak (carboxylate peak at 1540 and 1400 cm^{-1}). [45,46] The intensity of the strong amide peak at 1638 cm^{-1} (C=O) and 1540 cm^{-1} (N–H) in the annealed free-standing films indicates the formation of cross-linkage (the N–H peak of amide bonds was overlapped with the $–COO^-$ peak). In addition, an observed peak of asymmetric $–NH_3^+$ at 1624–1627 cm^{-1} in the films without annealing shifted to carbonyl stretching in CONH amide at 1638 cm^{-1} in the annealed films, which indicates that charged primary amines of PAH within the films react with carboxylic acids of PAA to form amide bonds by annealing at 180°C.

Protein adsorption performance.

The adsorption properties of PAA/PAH (35-bilayer) without annealing and free-standing PAA/PAH (35-bilayer) films were evaluated before and after immersion in fibrinogen solution (Figure 9). They were immersed in a conditioned Fibrinogen solution for 20 min at 37°C and then rinsed and dried those membranes three times in PBS solution. The amount of fibrinogen adsorption was then evaluated by measuring FT-IR and comparing it with the results before immersion. The FT-IR spectra of Fibrinogen alone are shown in Figure 9. There are five major peaks: amide I band (1655 cm^{-1}), amide II band (1540 cm^{-1}), assigned to the CH_2 deformation (1450 cm^{-1}), vibrations of the amino acid side chains (1390 cm^{-1}), and amide III bands (1240 cm^{-1}). Peak separation was performed for the strongest amide I band and amide II bands, and the ratio of the peak areas was evaluated. The formula used in this case is shown as follows (equation 1),

$$y = y_0 + \frac{A}{w\sqrt{\pi/2}} e^{-2\frac{(x-x_c)^2}{w^2}} \qquad \text{equation 1}$$

where y_0 is offset, x_c is the center of the peak, w is the width of the peak, and A is the area of the peak. The calculation of each peak was conducted in the FT-IR software. The peak area ratio of the amide I band and the amide II band for fibrinogen alone is (Area of amide I band)/(Area of amide II band) = A1/A2 = 1.33.

In the following, the protein adsorption properties of the free-standing membrane are evaluated by this ratio of amide I band/amide II band (A1/A2). For the PAA/PAH film (35-bilayer) on the substrate before heat treatment, the peak area ratios before and after immersion in

fibrinogen solution were A1/A2 = 0.38 and A1/A2 = 0.43, respectively. The small change in the peak area ratio and the small ratio of fibrinogen to fibrinogen alone suggested that the surface of the film before the free-standing treatment was difficult for the protein to adsorb. On the other hand, the A1/A2 of the PAA/PAH free-standing film (35-bilayer) changed from 0.60 to 1.15 before and after immersion in fibrinogen solution. The strength of the amide I band is enhanced after fibrinogen adsorption, as evidenced by the IR results for fibrinogen alone. Thus, the free-standing membranes in this study show remarkable adsorption of fibrinogen.

On strongly hydrophilic surfaces, proteins are resistant to adsorption, and solutions containing proteins are difficult to adsorb on strongly superhydrophobic levels due to their high liquid repellent properties.[47-50] The successfully fabricated free-standing film has a weak hydrophilic surface with a contact angle of 82°. Although the presence of more free carboxyl and hydroxyl groups on the surface inhibits the adsorption properties of the protein, in the preparation process of this study, thermal cross-linking produced an amide bond between the carboxyl group of PAA and the amino group of PAH, making the surface more prone to the adsorption of the protein.

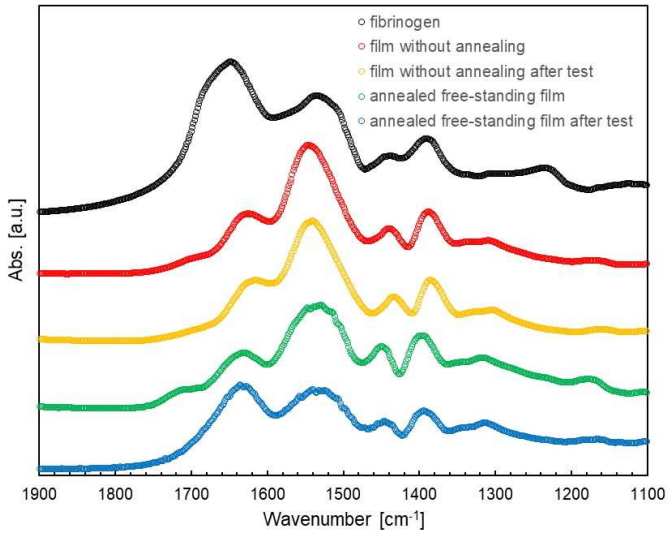

Figure 9. Fourier transform infrared spectra of fibrinogen, a LbL film before annealing, a LbL film before annealing after contact with a fibrinogen solution, a free-standing LbL film, and a free-standing LbL film after contact with a fibrinogen solution.

CONCLUSIONS

Here the study demonstrates wettability-controlled free-standing PAA/PAH films via LbL self-assembly with featuring each construction process. The surface wettability was controlled by changing the number of bilayers and the annealing temperature. About 10 min exfoliation time achieved the successful free-standing LbL films with 35-bilayer and annealing at 180°C. It showed a water contact angle of 82°, flexibility, and mechanical stability against the tensile testing. The free-standing PAA/PAH film trapped fibrinogen in the fibrinogen dispersion while the film without annealing did not show the change of peak ratio after the test. This study

suggests that the low wettable free-standing LbL films may enhance their fibrinogen adsorption property, leading to an improved wound healing process, being a potential material to recover the functional and structural properties of damaged skin.

ASSOCIATED CONTENT

AUTHOR INFORMATION

Corresponding Authors

Kengo Manabe – National Institute of Advanced Industrial Science and Technology (AIST), 1-2-1 Namiki, Tsukuba, Ibaraki 305-8564, Japan;

E-mail: kengo.manabe@aist.go.jp

Sabrina Belbekhouche – Institut de Chimie et des Matériaux Paris-Est, UMR 7182 CNRS-Université Paris-Est Créteil Val-de-Marne, 2 rue Henri Dunant, 94320 Thiais, France;

E-mail: belbekhouche@icmpe.cnrs.fr

Notes

The authors declare no competing financial interest.

ACKNOWLEDGMENT

A part of this research was conducted at the laboratory supported by Dr. Shiratori. We are also grateful to Mr. Hidefumi Nara, Mr. Motomi Matsuda, and Mr. Kohei Inoue, whose enormous support for the data collection and insightful comments were indispensable.

REFERENCES

[1] Pang, M., Huang, Y., Meng, F., Zhuang, Y., Liu, H., Du, M., Ma, Q., Wang, Q., Chen, Z., Chen, L., Cai, T., Cai, Y., 2020. Application of bacterial cellulose in skin and bone tissue engineering. Eur. Polym. J. 122, 109365. https://doi.org/10.1016/j.eurpolymj.2019.109365

[2] Sun, G., Zhang, X., Shen, Y.I., Sebastian, R., Dickinson, L.E., Fox-Talbot, K., Reinblatt, M., Steenbergen, C., Harmon, J.W., Gerecht, S., 2011. Dextran hydrogel scaffolds enhance angiogenic responses and promote complete skin regeneration during burn wound healing. Proc. Natl. Acad. Sci. U. S. A. 108, 20976–20981. https://doi.org/10.1073/pnas.1115973108

[3] Chen, T., Chen, Y., Rehman, H.U., Chen, Z., Yang, Z., Wang, M., Li, H., Liu, H., 2018. Ultratough, Self-Healing, and Tissue-Adhesive Hydrogel for Wound Dressing. ACS Appl. Mater. Interfaces 10, 33523–33531. https://doi.org/10.1021/acsami.8b10064

[4] Sousa, M.P., Neto, A.I., Correia, T.R., Miguel, S.P., Matsusaki, M., Correia, I.J., Mano, J.F., 2018. Bioinspired multilayer membranes as potential adhesive patches for skin wound healing. Biomater. Sci. 6, 1962–1975. https://doi.org/10.1039/c8bm00319j

[5] Qu, J., Zhao, X., Liang, Y., Zhang, T., Ma, P.X., Guo, B., 2018. Antibacterial adhesive injectable hydrogels with rapid self-healing, extensibility and compressibility as wound dressing for joints skin wound healing. Biomaterials 183, 185–199. https://doi.org/10.1016/j.biomaterials.2018.08.044

[6] Blacklow, S.O., Li, J., Freedman, B.R., Zeidi, M., Chen, C., Mooney, D.J., 2019. Bioinspired mechanically active adhesive dressings to accelerate wound closure. Sci. Adv. 5, 1–10. https://doi.org/10.1126/sciadv.aaw3963

[7] Yang, X., Yang, J., Wang, L., Ran, B., Jia, Y., Zhang, L., Yang, G., Shao, H., Jiang, X., 2017. Pharmaceutical Intermediate-Modified Gold Nanoparticles: Against Multidrug-Resistant Bacteria and Wound-Healing Application via an Electrospun Scaffold. ACS Nano 11, 5737–5745. https://doi.org/10.1021/acsnano.7b01240

[8] Perez, D., Bramkamp, M., Exe, C., von Ruden, C., Ziegler, A., 2010. Modern wound care for the poor: a randomized clinical trial comparing the vacuum system with conventional saline-soaked gauze dressings. Am. J. Surg. 199, 14–20. https://doi.org/10.1016/j.amjsurg.2008.12.029

[9] Zhao, X., Guo, B., Wu, H., Liang, Y., Ma, P.X., 2018. Injectable antibacterial conductive nanocomposite cryogels with rapid shape recovery for noncompressible hemorrhage and wound healing. Nat. Commun. 9. https://doi.org/10.1038/s41467-018-04998-9

[10] Li, M., Chen, J., Shi, M., Zhang, H., Ma, P.X., Guo, B., 2019. Electroactive anti-oxidant polyurethane elastomers with shape memory property as non-adherent wound dressing to enhance wound healing. Chem. Eng. J. 375, 121999. https://doi.org/10.1016/j.cej.2019.121999

[11] Yu, B., Kang, S.Y., Akthakul, A., Ramadurai, N., Pilkenton, M., Patel, A., Nashat, A., Anderson, D.G., Sakamoto, F.H., Gilchrest, B.A., Anderson, R.R., Langer, R., 2016. An elastic second skin. Nat. Mater. 15, 911–918. https://doi.org/10.1038/nmat4635

[12] Fang, Y., Zhu, X., Wang, N., Zhang, X., Yang, D., Nie, J., Ma, G., 2019. Biodegradable core-shell electrospun nanofibers based on PLA and γ-PGA for wound healing. Eur. Polym. J. 116, 30–37. https://doi.org/10.1016/j.eurpolymj.2019.03.050

[13] Zheng, K., Kapp, M., Boccaccini, A.R., 2019. Protein interactions with bioactive glass surfaces: A review. Appl. Mater. Today 15, 350–371. https://doi.org/10.1016/j.apmt.2019.02.003

[14] Guo, S., Zhu, X., Li, M., Shi, L., Ong, J.L.T., Jańczewski, D., Neoh, K.G., 2016. Parallel Control over Surface Charge and Wettability Using Polyelectrolyte Architecture: Effect on Protein Adsorption and Cell Adhesion. ACS Appl. Mater. Interfaces 8, 30552–30563. https://doi.org/10.1021/acsami.6b09481

[15] Wang, M., Zhang, Z., Wang, Y., Zhao, X., Yang, M., Men, X., 2019. Durable superwetting materials through layer-by-layer assembly: Multiple separations towards water/oil mixtures, water-in-oil and oil-in-water emulsions. Colloids Surfaces A Physicochem. Eng. Asp. 571, 142–150. https://doi.org/10.1016/j.colsurfa.2019.03.079

[16] Chandra, A., Bhuvanesh, E., Mandal, P., Chattopadhyay, S., 2018. Surface modification of anion exchange membrane using layer-by-layer polyelectrolytes deposition facilitating monovalent organic acid transport. Colloids Surfaces A Physicochem. Eng. Asp. 558, 579–590. https://doi.org/10.1016/j.colsurfa.2018.09.013

[17] Manabe, K., Kyung, K.H., Shiratori, S., 2015. Biocompatible slippery fluid-infused films composed of chitosan and alginate via layer-by-layer self-assembly and their antithrombogenicity. ACS Appl. Mater. Interfaces 7, 4763–4771. https://doi.org/10.1021/am508393n

[18] Manabe, K., 2020. Growth of porous chitin-nanofibrous structure via layer-by-layer self-assembly under existing ionic effects for antireflective and antifogging coatings. Prog. Org. Coatings 142, 105599. https://doi.org/10.1016/j.porgcoat.2020.105599

[19] Zhao, S., Caruso, F., Dahne, L., Decher, G., De Geest, B.G., Fan, J., Feliu, N., Gogotsi, Y., Hammond, P.T., Hersam, M.C., Khademhosseini, A., Kotov, N., Leporatti, S., Li, Y., Lisdat, F., Liz-Marzan, L.M., Moya, S., Mulvaney, P., Rogach, A.L., Roy, S., Shchukin, D.G., Skirtach, A.G., Stevens, M.M., Sukhorukov, G.B., Weiss, P.S., Yue, Z., Zhu, D., Parak, W.J., 2019. The Future of Layer-by-Layer Assembly: A Tribute to ACS Nano Associate Editor Helmuth Mohwald. ACS Nano 13, 6151–6169. https://doi.org/10.1021/acsnano.9b03326

[20] Poostforooshan, J., Belbekhouche, S., Shaban, M., Alphonse, V., Habert, D., Bousserrhine, N., Courty, J., Weber, A.P., 2020. Aerosol-Assisted Synthesis of Tailor-Made Hollow Mesoporous Silica Microspheres for Controlled Release of Antibacterial and Anticancer

Agents. ACS Appl. Mater. Interfaces 12, 6885–6898. https://doi.org/10.1021/acsami.9b20510

[21] Ariga, K., Ito, M., Mori, T., Watanabe, S., Takeya, J., 2019. Atom/molecular nanoarchitectonics for devices and related applications. Nano Today 28, 100762. https://doi.org/10.1016/j.nantod.2019.07.001

[22] Manabe, K., Matsubayashi, T., Tenjimbayashi, M., Moriya, T., Tsuge, Y., Kyung, K.H., Shiratori, S., 2016. Controllable Broadband Optical Transparency and Wettability Switching of Temperature-Activated Solid/Liquid-Infused Nanofibrous Membranes. ACS Nano 10, 9387–9396. https://doi.org/10.1021/acsnano.6b04333

[23] Ma, H., Li, S., Zhang, H., Wei, Y., Jiang, L., 2019. Fabrication of polydopamine-based layer-by-layer nanocomposites for combined pH-sensitive chemotherapy and photothermal therapy. Colloids Surfaces A Physicochem. Eng. Asp. 561, 332–340. https://doi.org/10.1016/j.colsurfa.2018.10.072

[24] Ariyarit, A., Manabe, K., Fukada, K., Kyung, K.H., Fujimoto, K., Shiratori, S., 2015. Semitransparent polymer-based solar cells via simple wet lamination process with TiO2 layer using automatic spray layer-by-layer method. RSC Adv. 5, 52427–52435. https://doi.org/10.1039/c5ra05762k

[25] Ji, Q., Qiao, X., Liu, X., Jia, H., Yu, J.S., Ariga, K., 2018. Enhanced adsorption selectivity of aromatic vapors in Carbon capsule film by control of surface surfactants on carbon capsule. Bull. Chem. Soc. Jpn. 91, 391–397. https://doi.org/10.1246/bcsj.20170357

[26] Hu, X., McIntosh, E., Simon, M.G., Staii, C., Thomas, S.W., 2016. Stimuli-Responsive Free-Standing Layer-By-Layer Films. Adv. Mater. 28, 715–721. https://doi.org/10.1002/adma.201504219

[27] Manabe, K., Nishizawa, S., Kyung, K.H., Shiratori, S., 2014. Optical phenomena and antifrosting property on biomimetics slippery fluid-infused antireflective films via layer-by-layer comparison with superhydrophobic and antireflective films. ACS Appl. Mater. Interfaces 6, 13985–13993. https://doi.org/10.1021/am503352x

[28] Nakamura, C., Manabe, K., Tenjimbayashi, M., Tokura, Y., Kyung, K.H., Shiratori, S., 2018. Heat-Shielding and Self-Cleaning Smart Windows: Near-Infrared Reflective Photonic Crystals with Self-Healing Omniphobicity via Layer-by-Layer Self-Assembly. ACS Appl. Mater. Interfaces 10, 22731–22738. https://doi.org/10.1021/acsami.8b05887

[29] Lee, H., Alcaraz, M.L., Rubner, M.F., Cohen, R.E., 2013. Zwitter-wettability and antifogging coatings with frost-resisting capabilities. ACS Nano 7, 2172–2185. https://doi.org/10.1021/nn3057966

[30] Manabe, K., Tanaka, C., Moriyama, Y., Tenjimbayashi, M., Nakamura, C., Tokura, Y., Matsubayashi, T., Kyung, K.H., Shiratori, S., 2016. Chitin nanofibers extracted from crab shells in broadband visible antireflection coatings with controlling layer-by-layer deposition and the application for durable antifog surfaces. ACS Appl. Mater. Interfaces 8, 31951–31958. https://doi.org/10.1021/acsami.6b11786

[31] Jiang, B., Zhang, H., Sun, Y., Zhang, L., Xu, L., Hao, L., Yang, H., 2017. Covalent layer-by-layer grafting (LBLG) functionalized superhydrophobic stainless steel mesh for

oil/water separation. Appl. Surf. Sci. 406, 150–160. https://doi.org/10.1016/j.apsusc.2017.02.102

[32] Manabe, K., Oniszczuk, J., Michely, L., Belbekhouche, S., 2020. pH- and redox-responsive hybrid porous CaCO3 microparticles based on cyclodextrin for loading three probes all at once. Colloids Surfaces A 602, 125072. https://doi.org/10.1016/j.colsurfa.2020.125072

[33] Mansour, O., El Joukhar, I., Belbekhouche, S., 2019. H_2O_2-sensitive delivery microparticles based on the boronic acid chemistry: (Phenylboronic –alginate derivative/dextran) system. React. Funct. Polym. 145, 104377. https://doi.org/10.1016/j.reactfunctpolym.2019.104377

[34] Ying, M., Sun, J., Shen, J., 2007. Ion-triggered exfoliation of layer-by-layer assembled poly(acrylic acid)/poly(allylamine hydrochloride) films from substrates: A facile way to prepare free-standing multilayer films. Chem. Mater. 19, 5058–5062. https://doi.org/10.1021/cm071260j

[35] Yang, J.M., Tsai, R.Z., Hsu, C.C., 2016. Protein adsorption on polyanion/polycation layer-by-layer assembled polyelectrolyte films. Colloids Surfaces B Biointerfaces 142, 98–104. https://doi.org/10.1016/j.colsurfb.2016.02.039

[36] Wittmer, C.R., Phelps, J.A., Saltzman, W.M., Van Tassel, P.R., 2007. Fibronectin terminated multilayer films: Protein adsorption and cell attachment studies. Biomaterials 28, 851–860. https://doi.org/10.1016/j.biomaterials.2006.09.037

[37] Wong, S.Y., Han, L., Timachova, K., Veselinovic, J., Hyder, M.N., Ortiz, C., Klibanov, A.M., Hammond, P.T., 2012. Drastically lowered protein adsorption on microbicidal hydrophobic/hydrophilic polyelectrolyte multilayers. Biomacromolecules 13, 719–726. https://doi.org/10.1021/bm201637e

[38] Quinn, A., Tjipto, E., Yu, A., Gengenbach, T.R., Caruso, F., 2007. Polyelectrolyte blend multilayer films: Surface morphology, wettability, and protein adsorption characteristics. Langmuir 23, 4944–4949. https://doi.org/10.1021/la0634746

[39] Matsuda, M., Shiratori, S., 2011. Correlation of antithrombogenicity and heat treatment for layer-by-layer self-assembled polyelectrolyte films. Langmuir 27, 4271–4277. https://doi.org/10.1021/la200340v

[40] Manabe, K., Matsuda, M., Nakamura, C., Takahashi, K., Kyung, K.H., Shiratori, S., 2017. Antifibrinogen, Antireflective, Antifogging Surfaces with Biocompatible Nano-Ordered Hierarchical Texture Fabricated by Layer-by-Layer Self-Assembly. Chem. Mater. 29, 4745–4753. https://doi.org/10.1021/acs.chemmater.7b00465

[41] Yoo, D., Shiratori, S.S., Rubner, M.F., 1998. Controlling bilayer composition and surface wettability of sequentially adsorbed multilayers of weak polyelectrolytes. Macromolecules 31, 4309–4318. https://doi.org/10.1021/ma9800360

[42] Qi, S., Li, W., Zhao, Y., Ma, N., Wei, J., Chin, T.W., Tang, C.Y., 2012. Influence of the properties of layer-by-layer active layers on forward osmosis performance. J. Memb. Sci. 423–424, 536–542. https://doi.org/10.1016/j.memsci.2012.09.009

[43] Bel'nikevich, N.G., Budtova, T. V., Vesnebolotskaya, S.A., Elyashevich, G.K., 2008. Effect of degree of cross-linking of sodium acrylate hydrogels on their swelling in variously acidic solutions. Russ. J. Appl. Chem. 81, 1818–1820. https://doi.org/10.1134/S1070427208100212

[44] Ma, Y., Zhang, Y., Wu, B., Sun, W., Li, Z., Sun, J., 2011. Polyelectrolyte multilayer films for building energetic walking devices. Angew. Chemie - Int. Ed. 50, 6254–6257. https://doi.org/10.1002/anie.201101054

[45] Shao, L., Lutkenhaus, J.L., 2010. Thermochemical properties of free-standing electrostatic layer-by-layer assemblies containing poly (allylamine hydrochloride) and poly (acrylic acid). Soft Matter 6, 3363–3369. https://doi.org/10.1039/c0sm00082e

[46] Park, J., Park, J., Kim, S. H., Cho, J. Bang, J., 2010. Desalination membranes from pH-controlled and thermally-crosslinked layer-by-layer assembled multilayers. J. Mater. Chem. 20, 2085–2091. https://doi.org/10.1039/b918921a

[47] Moradi, S., Hadjesfandiari, N., Toosi, S.F., Kizhakkedathu, J.N., Hatzikiriakos, S.G., 2016. Effect of Extreme Wettability on Platelet Adhesion on Metallic Implants: From Superhydrophilicity to Superhydrophobicity. ACS Appl. Mater. Interfaces 8, 17631–17641. https://doi.org/10.1021/acsami.6b03644

[48] Li, D., Wei, Q., Wu, C., Zhang, X., Xue, Q., Zheng, T., Cao, M., 2020. Superhydrophilicity and strong salt-affinity: Zwitterionic polymer grafted surfaces with significant potentials particularly in biological systems. Adv. Colloid Interface Sci. 278, 102141. https://doi.org/10.1016/j.cis.2020.102141

[49] Jokinen, V., Kankuri, E., Hoshian, S., Franssila, S., Ras, R.H.A., 2018. Superhydrophobic Blood-Repellent Surfaces. Adv. Mater. 30. https://doi.org/10.1002/adma.201705104

[50] Okamoto, R., Onuki, A., 2010. Precipitation in aqueous mixtures with addition of a strongly hydrophilic or hydrophobic solute. Phys. Rev. E 82, 1–20. https://doi.org/10.1103/PhysRevE.82.051501

“Table of co□te□ts o□ly”